



## Wound healing and blastema formation in regenerating digit tips of adult mice

Warnakulasuriya Akash Fernando, Eric Leininger, Jennifer Simkin, Ni Li, Carrie A. Malcom, Shyam Sathyamoorthi, Manjong Han, Ken Muneoka<sup>\*</sup>

Division of Developmental Biology, Department of Cell and Molecular Biology, Tulane University, 2000 Percival Stern Hall, New Orleans, LA 70118, USA

### ARTICLE INFO

#### Article history:

Received for publication 4 August 2010

Revised 2 November 2010

Accepted 27 November 2010

Available online 8 December 2010

#### Keywords:

Regeneration  
Wound healing  
Mouse  
Digit tip  
Blastema  
Osteoclast

### ABSTRACT

Amputation of the distal region of the terminal phalanx of mice causes an initial wound healing response followed by blastema formation and the regeneration of the digit tip. Thus far, most regeneration studies have focused in embryonic or neonatal models and few studies have examined adult digit regeneration. Here we report on studies that include morphological, immunohistological, and volumetric analyses of adult digit regeneration stages. The regenerated digit is grossly similar to the original, but is not a perfect replacement. Re-differentiation of the digit tip occurs by intramembranous ossification forming a trabecular bone network that replaces the amputated cortical bone. The digit blastema is comprised of proliferating cells that express vimentin, a general mesenchymal marker, and by comparison to mature tissues, contains fewer endothelial cells indicative of reduced vascularity. The majority of blastemal cells expressing the stem cell marker SCA-1, also co-express the endothelial marker CD31, suggesting the presence of endothelial progenitor cells. Epidermal closure during wound healing is very slow and is characterized by a failure of the wound epidermis to close across amputated bone. Instead, the wound healing phase is associated with an osteoclast response that degrades the stump bone allowing the wound epidermis to undercut the distal bone resulting in a novel re-amputation response. Thus, the regeneration process initiates from a level that is proximal to the original plane of amputation.

© 2010 Elsevier Inc. All rights reserved.

### Introduction

Amputation injury through the terminal phalanx of the mouse can result in an epimorphic regeneration response with near perfect restoration of morphology (Muneoka et al., 2008). Digit tip regeneration has also been documented in rats and monkeys (Said et al., 2004; Singer et al., 1987), and there is an extensive clinical literature demonstrating regeneration of human fingertips following amputation injury (Illingworth, 1974; see Muller et al., 1999). In mice, digit tip regeneration has been demonstrated in embryonic, neonatal and adult models (Borgens, 1982; Reginelli et al., 1995; Neufeld and Zhao, 1995). Regeneration is level-dependent; injury following amputation of the distal region of the third phalangeal element (P3) regenerates, whereas amputation injury at a more proximal level fails to regenerate (Neufeld and Zhao, 1995; Han et al., 2008). Mutant studies have identified the homeobox-containing gene, *Msx1*, as necessary for embryonic digit tip regeneration, and subsequent studies identified the BMP signaling pathway as downstream of *Msx1* and required for successful regeneration (Han et al., 2003). Studies on neonate digits show that BMP signaling is similarly required for successful regeneration, and that regeneration

from a proximal (non-regenerating) amputation injury can be stimulated by targeted treatment with BMP2 or BMP7 (Yu et al., 2010). Thus, the level-dependent regenerative ability of the mouse digit represents a model for characterizing endogenous regeneration, and also provides a gain of function approach (i.e. non-regenerating proximal amputation) that can be used to identify factors important for transitioning between wound healing and regeneration. In addition, because mouse digit tip regeneration is similar to clinically documented finger regeneration, these studies are directly relevant to the problem of human regeneration and regenerative medicine (Han et al., 2008; Muneoka et al., 2008).

The best characterized model for the regeneration of mammalian limb structures is the neonatal mouse digit (Han et al., 2008). Digit tip regeneration involves a slow and variable wound healing response resulting in the formation of a digit blastema containing proliferating cells that re-express a number of developmental genes associated with digit tip formation. Remarkably, bone formation during redifferentiation occurs by direct intramembranous ossification and the final regenerated bone is not a perfect replacement, never reaching the proximal–distal length of unamputated digits (Han et al., 2008). The imprecision of the final regenerate along with a mode of bone formation that deviates from endochondral ossification of digit development suggests that this injury response represents a case of evolved regeneration (Muneoka et al., 2008). The conclusion that mammals have evolved regenerative ability

<sup>\*</sup> Corresponding author. Fax: +1 504 865 6785.

E-mail address: [kmuneoka@tulane.edu](mailto:kmuneoka@tulane.edu) (K. Muneoka).

from a non-regenerating pre-condition has important implications for current strategies in regenerative medicine.

The neonatal digit tip has developed to a point where the basic structure is well established but is far from its final form. The neonatal digit tip is still actively involved in differentiating the proximal epiphyseal growth plate which does not close until postnatal day 21 (Muneoka et al., 2008). In addition, the digit tip continues to elongate by appositional ossification until it reaches its final size at 8 weeks of age (Han et al., 2008). Because of the maturity of digit tissues, the amputated adult digit stump represents a significantly different injury model, yet it is able to undergo a similar regenerative response (Borgens, 1982; Neufeld and Zhao, 1995; Revardel and Chebouki, 1986). The regeneration of the adult digit displays a level-dependent response similar to neonates (Neufeld and Zhao, 1995), and direct ossification during redifferentiation has been noted (Muller et al., 1999). The purpose of this study is to provide a detailed and quantitative description of the adult digit tip regeneration response. Of note, our studies reveal 1) a wound healing phase that is dominated by the extensive degradation of the stump bone, associated with an enhanced presence of osteoclasts, prior to blastema formation, 2) the formation of a blastema that has a reduced level of endothelial cells in conjunction with a reduced vasculature, and 3) an imprecise redifferentiation process that produces larger regenerates.

## Materials and methods

### *Amputations and animal handling*

All animals used for the experiments were adult female CD1 mice (8–10 weeks old) obtained from Charles River laboratories (Wilmington, MA) or Harlan laboratories (Indianapolis, IN). Mice were anesthetized with Ketamine/Xylazine (Ketamine 80 mg/kg, Xylazine 8 mg/kg, IP). The second and fourth digits of the hind limbs were used for amputations. Regenerating digits were collected between 5 and 128 days post amputation (DPA), imaged to assess external anatomy and processed for histology. For morphological studies, a sample size of at least 6 digits was used for each time point. All experiments were performed in accordance with the standard operating procedures approved by the Institutional Animal Care & Use Committee of Tulane University Health Science Center.

### *Histology and immunohistochemistry*

The digits were fixed in zinc buffered formalin (Z-fix, Sigma) and decalcified in Decalcifier II (Surgipath, Richmond, IL) for histological analysis. Digits were dehydrated, embedded in paraffin, serially sectioned (sagittal, 6–8 microns), and stained with Mallory's triple stain as previously described (Han et al., 2008). Length measurements were taken from mid-sagittal sections of digits from 5 different animals for each time point.

Immunohistochemistry studies were carried out on fresh frozen sections prepared at 4  $\mu$ m using a Cryo-Jane tape transfer system as describe by the manufacturer (Instrumedics). Tissue sections were fixed in cold acetone for 10 minutes, washed in PBS, blocked with 10% BSA, 0.1% Tween20, and incubated with primary antibody for 1.5 hours at room temperature. Primary antibodies used were rat anti-mouse Ki67 (Dako), rat anti-mouse SCA-1 conjugated to Alexa 488 (Bio Legend), rat anti-mouse CD31 conjugated to Alexa647 (Bio Legend), and chicken anti-vimentin (Millipore). For secondary antibodies we used goat anti-rat-Alexa 647 (Invitrogen) for Ki67, and goat anti-chicken-Alexa 568 (Invitrogen) for vimentin. Slides were washed with PBS, stained with DAPI (Invitrogen), and mounted with Prolong (Invitrogen). One digit each from three different animals was analyzed. For each digit we analyzed three nonadjacent sections through the central region of the digit. The areas analyzed were the

dorsal connective tissue closest to the amputation plane and the bone marrow at the time of injury, and the entire blastema at 10 days post amputation. All cell counts were performed with 400 $\times$  magnification, and the frequencies were calculated by counting labeled cells and dividing by the total number of DAPI stained nuclei within a field of view.

### *TRAP staining method*

For tartrate resistant acid phosphatase staining (TRAP) samples were fixed in zinc-buffered formalin for 48 hours and decalcified with 8% formic acid in 10% formaldehyde (Surgipath) for 8 hours. The samples were dehydrated through an ethanol series, embedded in paraffin and sectioned. After deparaffinization, 4  $\mu$ m thick sections were incubated in buffered Naphtol-AS-BI-phosphate/Fast Red Violet LB (pH 5.2) with 50  $\mu$ M sodium tartrate (Takara Bio Inc) for 4 hours at 37  $^{\circ}$ C. Slides were counterstained with Mayer's Hematoxylin, developed in running tap water for 10 minutes, dehydrated and mounted.

### *Micro-computed tomography (MicroCT)*

Mice were anesthetized and maintained with isoflurane for longitudinal X-ray and microCT studies of digit tip regeneration ( $N=8$ ). X-ray images were obtained every 2–3 days using the scout view positioning function of a Scanco vivaCT-40 and full scans (55 kVp at 12.5  $\mu$ m) were carried out on days 9, 18 and 28. For quantitative volumetric analysis digits were collected at selected time points, fixed overnight in Z-fix, and washed with 100% ethanol. Digits were then placed in alcoholic iodine overnight in order to increase soft-tissue contrast (Metscher, 2009). This treatment made the epidermis radio-opaque allowing subsequent region of interest (ROI) selection of the non-opaque connective tissue that was adjacent to the nail and between the bone and epidermis. Digits were then washed and imaged (45 kVp at 10.5 or 15  $\mu$ m). Serial sections were exported into SanteDicom Editor where volume measurements of bone and connective tissue were reconstructed frame by frame with ROI tools. These voxel measurements were subsequently exported and tallied in Microsoft Excel 2007. 3-D images and visualization of serially reconstructed digit slices were done using Vol-View (Kitware Inc.). A sample size of 3 digits was analyzed for each timepoint.

### *Statistics and analysis*

Osteoclasts were identified histologically as large multinucleated cells associated with bone tissue. For quantification three non-adjacent sections from four different digits, from four different animals were analyzed. The bone area was measured using Photoshop CS4 software, and the total number of osteoclast cells per square millimeter area of bone was calculated as described (Bolon et al., 2004). ANOVA statistics and standard error were calculated using Instat 3.06 (Graphpad) software for all measurements. All graphs and images were published and created in Igor Pro 5 (Wavemetrics), and Microsoft excel.

## Results

### *External changes during digit tip regeneration*

Histological stages during adult digit tip regeneration have been previously described for amputations midway through the digit tip including the distal part of the fat pad of forelimb digits in Swiss mice (Revardel and Chebouki, 1986). Unlike this previous model, our digit tip regeneration model is restricted to amputation of the distal region of P3 without injury to the fat pad of the hindlimb digit in CD1 mice, and is similar to neonatal amputations that have been well characterized (Han et al., 2008). Nevertheless, our anatomical

observations are largely in parallel with this previous report. In addition to documenting histological changes during the regeneration response, our characterization of terminal phalanx regeneration includes gross morphological changes, volumetric changes derived from MicroCT scanning, and an immunohistochemical assessment of re-vascularization of the blastema.

The terminal phalanx of the adult mouse consists of a triangle shaped bone encased within a nail organ that curves ventrally at the digit tip, and a fat pad located ventrally at the base of the bone (Fig. 1B). Externally, the translucent nail plate allows for the visualization of the distal region of the terminal phalangeal bone (Fig. 1A) and gross anatomical changes associated with bone

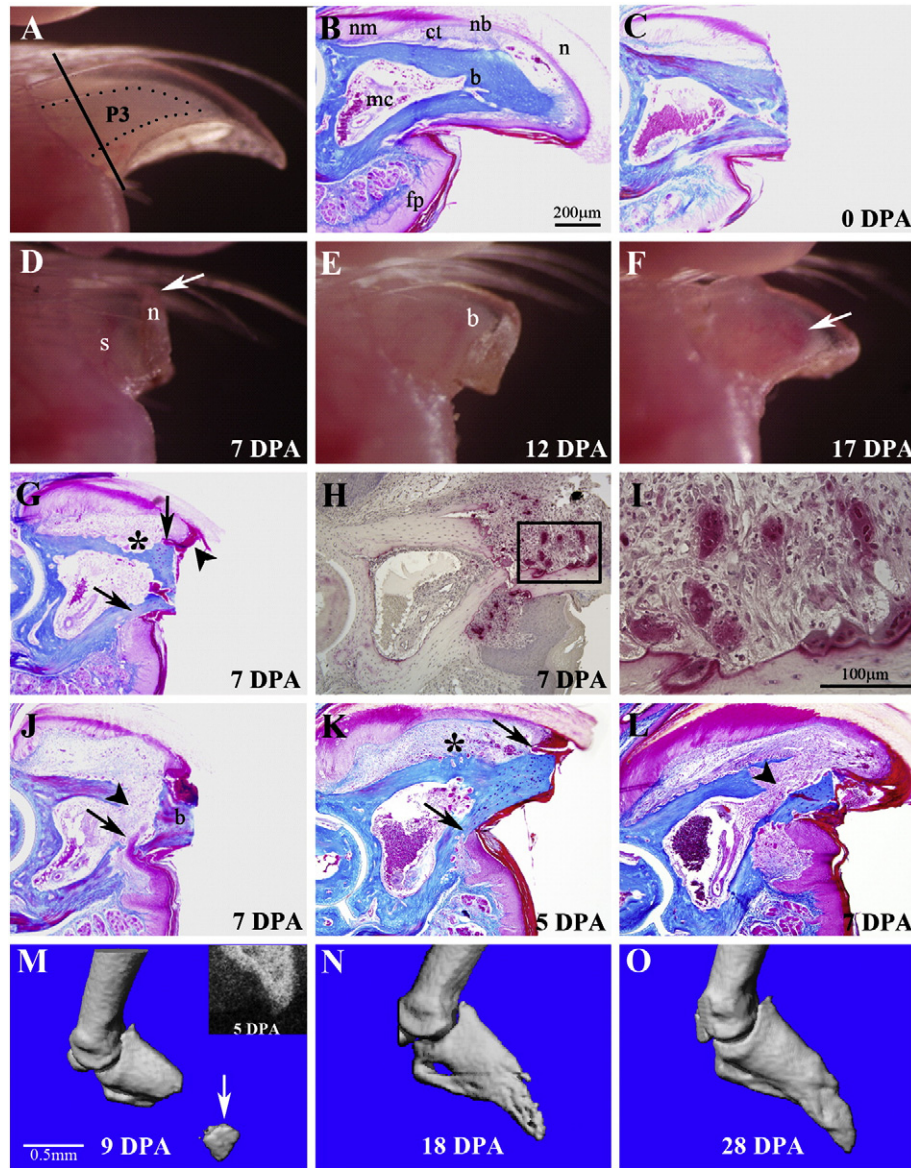


**Fig. 1.** External morphology and wound healing during adult digit tip regeneration. (A) The distal region of the adult digit tip is comprised of the tip of the P3 skeletal element (outlined) that is visible through the opaque nail plate, the surrounding connective tissue and the nail plate. The plane of amputation is indicated by the solid line. (B) Sagittal section through an unamputated digit tip shows a triangle shaped bone (b) that tapers to a pointed tip and with a bone marrow cavity (mc) localized in the proximal region. A thin band of connective tissue (ct) that is more prominent dorsally surrounds the P3 bone. Epidermal derivatives include the proximal multi-layered nail matrix (nm) that extends distally into the nail bed (nb) and underlying the nail plate (n). The digit fat pad (fp) is located ventrally in the proximal region of the digit tip. (C) Sagittal section of the digit tip immediately after amputation. Amputation is made through the distal cortical bone and nail bed, but leaves the marrow cavity intact. (D) External view of a regenerating digit tip at 7 DPA showing distal elongation (arrow) of the nail plate (n), with no remarkable change of the stump bone (s). (E) External view of a regenerating digit tip at 12 DPA showing outgrowth of a prominent digit blastema (b). (F) External view of a regenerating digit tip at 17 DPA showing a regenerate that has the general shape of the terminal phalanx. Vasculature associated with ossification is visible through the nail plate (arrow). (G) Histological section of a regenerating digit at 7 DPA showing an increase in the connective tissue dorsal to the bone, epidermal attachment to the dorsal and ventral bone surfaces (arrows), and distal overgrowth of the dorsal epidermis (arrowhead). Significant bone degradation (\*) is observed at this stage. (H) TRAP staining of 7 DPA regenerates identifies osteoclasts that are specifically localized to the amputated stump. (I) Higher magnification of the region within the box in H showing some osteoclasts directly associated with bone and other osteoclasts that appear to be within the wound mesenchyme. (J) Histological section of a regenerating digit at 7 DPA showing epidermal migration (arrow) through a region of eroded stump bone. This mode of wound closure causes a re-amputation and sloughing of the amputated bone (b). Bone erosion opens the distal region of the marrow cavity (arrowhead) allowing marrow-derived cells to enter the wound. (K) Amputation at the very distal digit tip creates a very small amputation wound. At 5 DPA the epidermis remains attached to the dorsal and ventral bone surfaces (arrows) and there is evidence of bone erosion (\*) at the level of the marrow cavity. (L) In very distal amputations at 7 DPA, wound closure is still incomplete, the bone enclosing the marrow cavity is completely eroded and the marrow cavity is contiguous with the amputation wound (arrowhead). (M–O) Longitudinal imaging of a regenerating digit tip. (M) MicroCT scan at 9 DPA shows a re-amputated distal bone fragment (arrow) prior to being sloughed off. An X-ray image of the digit tip at 5 DPA (inset) shows the distal bony stump and an intact marrow cavity. (N) MicroCT scan at 18 DPA shows the regenerated digit tip is nearly complete. (O) MicroCT scan at 28 DPA showing the digit tip completely regenerated digit.



formation during later stages of regeneration (Fig. 1E and F). The proximal region of the terminal phalanx expands to form the base of the triangular bone where it articulates with the distal end of the second phalangeal element (P2). The P3 element has a marrow cavity located proximally that tapers toward the distal tip, and with the exception of the joint region, the bony tissue is dense cortical bone (Fig. 1B).

Digit tip amputations are made distal to the ventral fat pad, removing the distal region of P3 and surrounding tissues, including nail and loose connective tissues (Fig. 1C). The amputation stump consists of the nail plate, nail bed (epidermis underlying the nail dorsally and laterally), ventral epidermis, and loose connective tissue surrounding cortical bone. The marrow cavity is not exposed to the amputation plane and while there is some blood loss, the clotting response is rapid. During the first week post-amputation the only remarkable change in external morphology is the continued outgrowth of the nail plate that extends distal to the plane of amputation (Fig. 1D). During the second week post-amputation an opaque mass of cells that extends distal to the amputation plane is visible through the nail plate (Fig. 1E). By 17 DPA, a regenerated conical shaped digit tip is visible (Fig. 1F).

### Wound healing

Digit tip amputation transects the nail bed but not the marrow cavity, and exposes a surface of cortical bone in the amputation wound. There are canals within the distal region of the P3 bone that connect the marrow cavity to the external bone surface and these canals are generally transected by amputation (Fig. 1C). Approximately 30% of the proximal–distal length of the P3 bone is removed by amputation. There are a number of remarkable changes to the digit stump during the first week of wound healing. First, the number of cells in the stump connective tissue is enhanced and is likely linked in part to an inflammation response. Second, we have not observed epidermal closure of the wound over the amputated bone in any sample examined, thus we conclude that it does not occur. During this period the epidermis associated with the nail plate remains connected to the lateral surface of the stump bone at the level of amputation (Fig. 1G). On the ventral side where the epidermis is not associated with the nail plate, the epidermis retracts proximally and is connected to the external bone surface at a level of the marrow cavity. Thus, closure of the amputation wound is inhibited by the stump bone.

The third remarkable change of the digit stump is the extensive degradation of the stump bone proximal to the amputation plane. The timing of bone degradation is variable from digit to digit; however, it occurs in all amputated digits and is regionally restricted to a level associated with the distal bone marrow cavity. Regions of bone erosion are associated with the presence of large multinucleated cells on both the endosteal and periosteal surfaces of the bone and these cells are identified as osteoclasts based on morphology and TRAP staining (Fig. 1H, I). It is well established that osteoclasts function in bone resorption (Vaananen et al., 2000), so we conclude that they are responsible for the bone degradation response we see in digit regeneration. Consistent with this conclusion, cell counts indicate that osteoclasts are rare in the unamputated digit tip, increase during wound healing stages (3 cells/mm<sup>2</sup> of bone area at 7 DPA), decrease by blastema formation (0.5 cells/mm<sup>2</sup> of bone area at 10 DPA) and are scarce in the regenerate. In the absence of epidermal closure across the amputated bone stump, this rapid degradation of stump bone provides an epidermal migration route that undercuts the distal bone stump (Fig. 1J). This results in the sloughing of the distal bone stump and effectively re-amputates the digit tip at a more proximal level. We note that this self-amputation always cuts through to the marrow cavity and exposes marrow cells to the wound site (see arrowhead in Fig. 1J).

The absence of wound closure over amputated bone and the extensive erosion of bone during wound healing raised the question of whether wound closure would occur over a very small amputated bone surface. Since the digit tip tapers to a point we carried out extreme distal amputations in which only the very tip of the bone was amputated. Histological analyses after 5 days (Fig. 1K) indicated that wound closure does not occur over these minimal amputations. Instead, the ventral epidermis retracts proximally to the level of the marrow cavity while the dorsal epidermis remains at the distal amputation plane. At 5 DPA there is evidence that bone degradation initiates at the level of the marrow cavity both dorsally (\* in Fig. 1K), and ventrally, in association with the healing edge of the ventral epidermis (arrow in Fig. 1K). By 7 DPA the bone enclosing the marrow region is eroded allowing cells within the marrow to spill out into the amputation wound (Fig. 1L). These extreme distal amputations result in bone erosion with wound closure occurring through regions of eroded bone resulting in a secondary amputation at a more proximal level.

We used microCT analysis to explore the frequency and timing of this bone degradation response. We documented the regeneration response of 8 digit tip amputations gathering X-ray images every 2–3 days and carrying out a microCT scan at 9- to 10-day intervals. The data indicate that bone degradation is associated with a re-amputation response in all 8 digits; however the timing of this response varied among the digits. In 50% of the digits analyzed the re-amputation was completed by 9 DPA whereas the remaining 50% completed re-amputation by 12 DPA. A representative longitudinal series of X-ray and microCT scans from a single regenerating digit tip in which re-amputation occurred prior to 9 DPA is shown (Fig. 1M–O). The X-ray image at 5 DPA shows an intact marrow cavity of the amputated digit tip prior to re-amputation (Fig. 1M, inset), and the microCT scan at 9 DPA shows a re-amputated stump bone (arrow) prior to being sloughed off (Fig. 1M). 9 days later (18 DPA) the regenerating digit tip is nearly complete (Fig. 1N), and regeneration is complete by 28 DPA (Fig. 1O).

### Blastema formation

Wound closure time during digit tip regeneration is variable and is related to the bone degradation response. Once re-epithelization of the wound occurs however, there is a tight relationship between the timing of wound closure and the formation of a digit blastema. The time to complete wound closure was determined by analyzing serially sectioned digits at multiple timepoints (Table 1). By 8 DPA wound closure was complete in only 1 of 9 digits and that digit had initiated blastema formation. By 10 DPA wound closure was complete in 6 of 9 digits and all 6 of these digit possessed prominent blastemas (see Fig. 3A). By 12 DPA all digits analyzed had closed their wounds and all digits had prominent blastemas. Thus, soon after completing wound closure the wound site undergoes a dramatic transformation to generate the digit blastema. Although there is considerable variability, this transformation generally occurs between 8 and 10 days after amputation. Because of the degradation and sloughing of the stump bone, the blastema that forms is at a level proximal to the original amputation plane. The base of the blastema is always contiguous with both the marrow cavity centrally and the loose connective tissue peripherally.

**Table 1**  
Epidermal closure and blastema formation.

DPA	Epidermal closure	Blastema formation	Ossification
0 (N = 6)	0/6	0/6	0/6
7/8 (N = 9)	1/9	1/9	0/9
10 (N = 9)	6/9	6/9	0/9
12 (N = 6)	6/6	6/6	1/6

Enhanced cell proliferation is the hallmark of blastema formation. The proliferation of blastema cells was analyzed in samples at 10 DPA based on immunostaining with the cell proliferation marker Ki67. Ki67<sup>+</sup> cells were identified in non-adjacent sagittal sections throughout the blastemas of 3 digits. The frequency of Ki67 positive blastema cells was compared to similar counts taken from the dorsal connective tissue and cells within the bone marrow of digit tips fixed immediately after amputation. The labeling index of cells in the blastema (7.70%) was found to be enhanced 8-fold over non-regenerating digit tip connective tissue (0.92%) and 4-fold over cells within the P3 bone marrow (1.77%). We also found that virtually all blastema cells, but not cells of the wound epidermis, stained positive for the general mesenchymal marker vimentin (Kalluri and Zeisberg, 2006) (Fig. 2A, D). Vimentin is also expressed in many cells of the connective tissue and bone marrow, but not the epidermis, of the digit stump immediately after amputation (Fig. 2E, H, L).

The regenerating digit has been shown to have a reduced level of vascularization by comparison to healed non-regenerating digit amputation injuries (Said et al., 2004). To explore the issue of vascularization during regeneration we carried out immunohisto-

chemical studies using anti-CD31 (PECAM-1), an established marker for endothelial cells (Newman et al., 1990; Woodfin et al., 2007), to characterize the involvement of endothelial cells in digit blastema formation. For comparison, CD31<sup>+</sup> cells were counted in the connective tissue of the stump and in the P3 bone marrow immediately after amputation of the digit tip. The expression of CD31 is prominent in both connective tissue (Fig. 2F) and bone marrow (Fig. 2J) of the digit stump, representing 16.2% of all connective tissue cells and 22.1% of all cells within the bone marrow (Fig. 2I). In addition, the majority of CD31 positive cells were associated with histologically identifiable vascular structures indicating that these cells are endothelial. By 10 DPA in digits that have a prominent blastema, the expression of CD31 remains high in the stump region, but there is a significant decline in the frequency of CD31<sup>+</sup> cells within the blastema (Fig. 2B, I; 10.2%). Consistent with previous observations, few vessels are observed in the blastema and the majority of CD31 positive cells were individual elongated cells scattered throughout the blastema. These results indicate that blastema formation is associated with a relative decline in endothelial cells associated with re-vascularization.

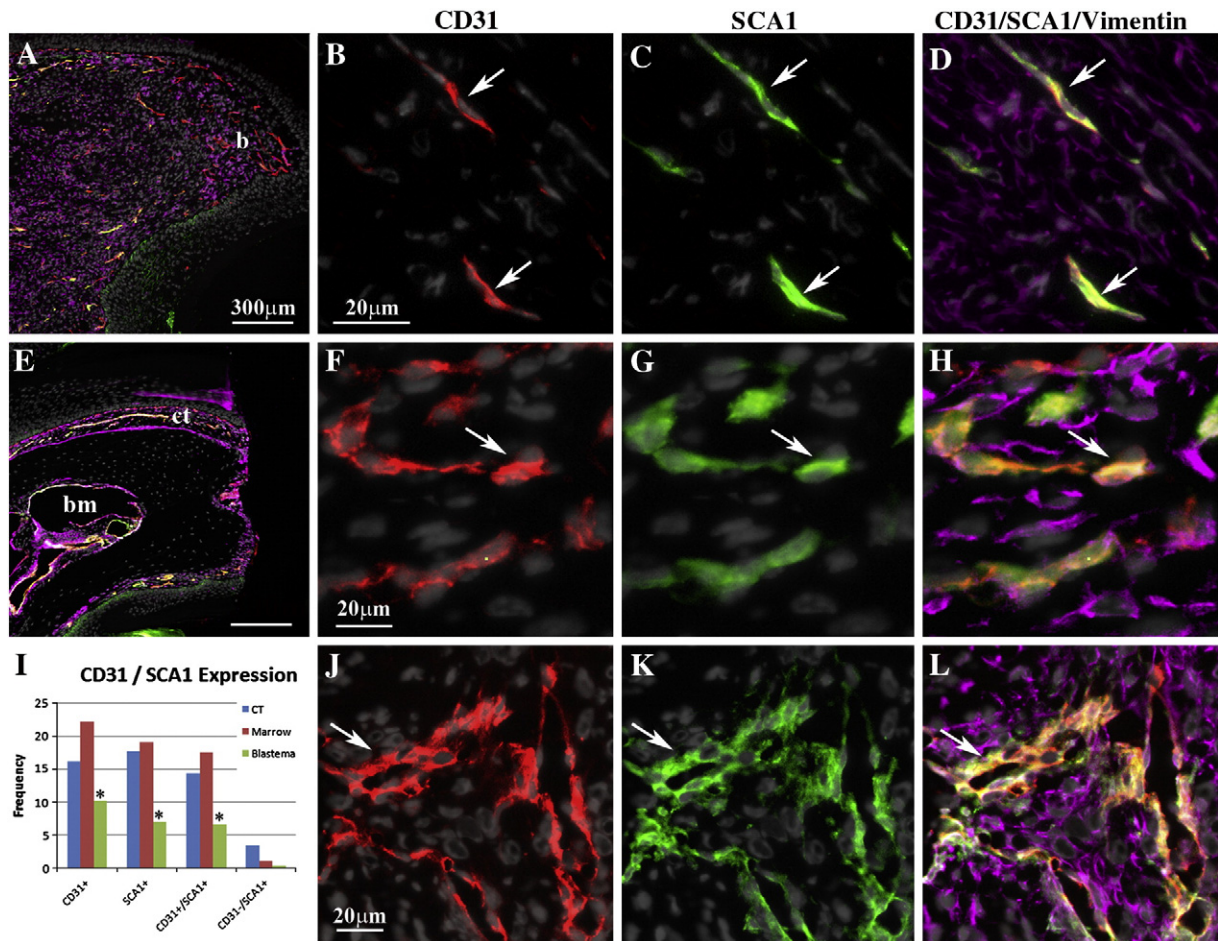


**Fig. 2.** Blastema Formation. (A) Low magnification image of a sagittal section of a 10 DPA blastema (b) stained with DAPI and immunostained for vimentin (purple), CD31 (red) and SCA-1 (green). Distal is to the right and dorsal is the top. (B–D) High magnification image of the blastema stained with DAPI to identify nuclei, and immunostained for the endothelial cell marker, CD31, the stem cell marker, SCA-1, and the mesenchymal marker, vimentin. CD31 specific staining is shown in B, SCA-1 specific staining is shown in C, and staining with all markers is shown in D. Arrows indicate endothelial progenitor cells that co-express CD31 and SCA-1. (E) Low magnification image of a sagittal section through the digit stump immediately after amputation. Distal is to the right and dorsal is the top. The section is stained with DAPI and immunostained for vimentin, CD31 and SCA-1. The stump bone and epidermis display no immunoreactivity, whereas there is extensive expression by cells of the connective tissue (ct) surround the bone stump and the bone marrow (bm). (F–H) High magnification image of the dorsal connective tissue stained with DAPI, and immunostained with CD31, SCA-1, and vimentin. CD31 specific staining is shown in F, SCA-1 specific staining is shown in G, and staining with all markers is shown in H. The arrow indicates one of many endothelial progenitor cells that co-express CD31 and SCA-1. (I) Cell counts indicate that the number of blastema cells (green columns) expressing CD31, SCA-1 and both CD31 and SCA-1 is reduced by comparison to the connective tissue (blue columns) and cells in the marrow cavity (red columns) of the digit. The number of SCA-1<sup>+</sup>/CD31<sup>+</sup> cells (far right) are most prevalent in the connective tissue (blue column) and least abundant in the blastema (green column). (J–L) High magnification image of the stump bone marrow stained with DAPI, and immunostained with CD31, SCA-1, and vimentin. CD31 specific staining is shown in F, SCA-1 specific staining is shown in G, and staining with all markers is shown in H. The arrow indicates one of many endothelial progenitor cells that co-express CD31 and SCA-1.



SCA-1 is a cell surface marker associated with a variety of stem cells including hematopoietic stem cells, mesenchymal stem cells and endothelial stem cells (Holmes and Stanford, 2007). A recent study on non-regenerating digit amputation injury reported the accumulation of SCA-1 positive cells associated with the wound healing response (Agrawal et al., 2009). We used immunohistochemistry to characterize the involvement of cells expressing SCA-1 in the regeneration response. SCA-1 is expressed by many cells in the connective tissue (17.7%) and bone marrow (19.1%) of the digit tip at the time of amputation (Fig. 2G, I, K). In contrast, only 7.0% of the blastema cells were positive for SCA-1 (Fig. 2C, I), thus blastema formation is associated with a relative reduction of SCA-1 expressing cells. Many of the SCA-1 positive cells in mature digit tissue appeared to be associated with the digit vasculature, so we carried out double immunostaining with anti-CD31 (Fig. 2D, H, L) to identify potential endothelial progenitor cells (Orimo et al., 2005). We found that 88.9% of the CD31 positive cells of the connective tissue, and 79.9% of the CD31 positive cells in the bone marrow co-expressed SCA-1 (see Fig. 2I), suggesting a high frequency of endothelial progenitor cells in the uninjured digit tip. Within the blastema 64.7% of the CD31 positive cells also expressed SCA-1 and they appeared to be localized to the very distal regions of the blastema. These data suggest that the majority of endothelial cells present in both the digit stump and in the regenerating digit blastema are endothelial progenitor cells.

SCA-1 expression is associated with a number of different adult stem cell populations so we reasoned that those SCA-1 positive cells that did not co-express CD31 in the blastema would provide evidence for the involvement of other stem cells in digit tip regeneration. SCA-1 positive cells in the blastema only 5.7% (0.4% of all blastema cells) of these cells were CD31 negative (Fig. 2I). Thus, while we cannot exclude the involvement of other stem cell populations, the involvement of SCA-1 positive cells in adult digit tip regeneration appears to be largely restricted to the endothelial lineage.

#### Re-differentiation during digit tip regeneration

Histological evidence for bone re-differentiation during digit tip regeneration was not observed in regenerates examined at 10 DPA ( $N=9$ ) or earlier, was found in 1 of 6 samples examined at 12

DPA, and in all samples examined at 17 DPA ( $N=6$ ) and later (Fig. 3A–C). Ossification is first seen at the interface between the stump bone and the base of the blastema (Fig. 3B). We found no histological evidence of chondrocytes during digit tip regeneration, indicating that the adult regeneration response involves direct ossification similar to that shown for neonatal regeneration (Han et al., 2008). The re-differentiation of newly regenerated bone progresses in a proximal to distal direction with new bone forming just distal to existing stump bone, but not in regions associated with the surrounding connective tissue or the central bone marrow. At 17 DPA all digits analyzed had differentiated a proximal cap of trabecular bone that is contiguous with the stump bone and encloses the marrow region (Fig. 3C). At this stage there is still a digit blastema distally. The general anatomy of the P3 element is essentially restored by 28 DPA with roughly the distal half of the element comprised of newly regenerated trabecular bone (Fig. 3D). The marrow maintains a connection with the intratrabecular spaces that form during intramembranous ossification and extends throughout the regenerated bone. After 28 days, ossification of the regenerated bone continues so that by 128 days the density of the regenerated bone is much enhanced and the intratrabecular network is reduced although still apparent (Fig. 3E). The overall pattern of the regenerated digit tip is generally similar to the unamputated digit; however, the regenerate can be distinguished from the stump based on histological differences between the cortical bone of the stump and the trabecular bone of the regenerate.

To provide a quantitative assessment of the regeneration response we analyzed serial sagittal sections of regenerating digits to obtain measurements of the proximal–distal length of the P3 bone at different stages as compared to the total proximal–distal length of the mesenchymal component of the digit (measured to the base of the distal epidermis, Fig. 3F). Based on this analysis we find that 1) approximately 30% of the P3 length was amputated, 2) the stump length is reduced by an additional 23% during wound healing and blastema formation, 3) the total length of the digit was restored by 17 DPA, and 4) that the proximal–distal length of the P3 element was restored by 28 DPA. These histological results along with detailed observations of gross anatomical changes identify a general series of

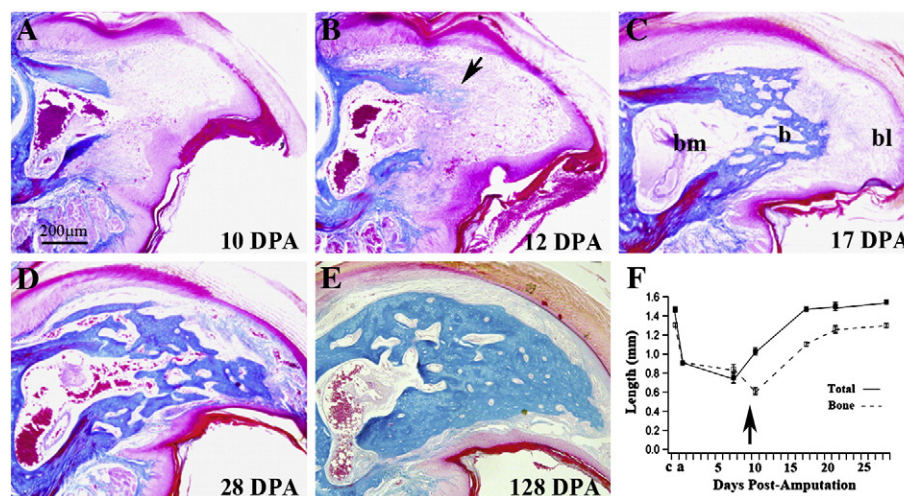


**Fig. 3.** Re-differentiation. Mid-sagittal histological sections of the regenerating digit tip stained with Malory's triple stain. (A) 10 DPA blastema shows no histological evidence of differentiation. (B) Direct ossification (arrow) was first observed in 1 of 6 samples analyzed at 12 DPA. (C) At 17 DPA all sample had regenerated new trabecular bone (b) that capped the distal region of the bone marrow cavity (bm) proximal to the digit blastema (bl). (D) At 28 DPA the distal region of P3 is regenerated with an interlacing network of new trabecular bone that is histologically distinct from the original cortical bone, but anatomically similar to the origin. Connective tissue has differentiated distally and there is no histological evidence of a blastema. (E) The 128 DPA regenerated digit tip has maintained the general digit structure but the bone density is increased relative to the early regenerate. (F) Graph showing the normalized longitudinal lengths of the digit tip (solid boxes) and the P3 bone (open boxes) during the regeneration process. The arrow highlights the relationship between bone erosion and blastema formation. Both total digit and P3 length regenerates to normal levels within 3–4 weeks. c, control digit length, a, amputated digit length.

stages that include wound healing (0–7 DPA), blastema formation (7–12 DPA) and re-differentiation (12–28 DPA). However, because of sample to sample variability, and as well the potential for strain variability, the use of time after amputation is not an ideal determinant of regeneration stages.

#### MicroCT analysis of adult digit tip regeneration

We carried out MicroCT analyses of selected regeneration stages as a non-invasive way to determine regeneration stages, and to characterize volumetric changes of bone and soft tissue that occur during the regenerative response. Bone tissue is readily visible in X-rays and bone volume can be estimated from MicroCT scans. In this study we analyzed fixed samples of intact and regenerating digit tips treated with iodine to make the epidermis radio-opaque (Fig. 4A), thus allowing for volume measurements of the soft tissue lying between the bone and epidermis. By subtracting bone volume from total volume in these samples we are able to quantitate changes in both bone and soft tissue during the regeneration process. The unamputated adult digit tip in Fig. 4A shows the triangular terminal phalangeal bone articulating proximally with the distal head of the P2 bone and the ventrally associated sesamoid process. The marrow cavity is located in the proximal region and is contiguous with the ventral bone canal (os hole) that provides a direct interface between the marrow and the surround soft tissues. After amputation of the distal tip, measurements of soft tissue and bone volume indicate that approximately 10% of the total tissue volume and 6.4% of the bone volume was removed by amputation (Fig. 4B, F). At the blastema stage (10 DPA) when outgrowth is first evident, there is a rise in the total tissue volume that involves a sharp increase in soft tissue volume (i.e. blastema formation) concomitant with a decrease in bone volume (Fig. 4C, G). The decrease in bone volume results in a stump bone that is 47% of the original P3 volume and MicroCT scans show clear evidence of bone degradation proximally to the level of the marrow cavity (Fig. 4C). These findings are consistent with the histological evidence of injury induced bone regression previously described (see Fig. 1G–J). Thus, the amount of bone loss caused by the initial

amputation is small by comparison to the injury-induced bone loss that occurs during wound healing. Between 10 and 17 DPA both the soft tissue volume and the bone volume increase resulting in a peak in total tissue volume that is roughly twice the total volume of the unamputated digit (Fig. 4D, F). Since the proximal–distal length of the regenerate returns to normal by this time (see Fig. 3E), the increase in volume must be linked to an increase in the girth of the regenerate. By 28 DPA when the regenerative process is largely complete the total tissue volume is reduced however it does not return to normal levels. Instead, the regenerated volume is roughly 25% higher than the original unamputated digit. Between 17 DPA and 28 DPA the bone volume remains relatively constant, but the final bone volume of the 28-day regenerate is significantly higher than the unamputated digit tip (Fig. 4F). When the ratio of the soft tissue volume (STV) to bone volume (BV) is normalized and plotted as a function of regeneration stage, blastema formation is associated with a 4-fold increase in STV:BV ratio and the re-differentiation phase results in the return of the STV:BV ratio to normal levels (Fig. 4G). Thus, while the total regenerated tissue volume is enhanced, the proximal–distal length (Fig. 3E) and the STV:BV ratio regenerate back to normal levels.

#### Discussion

Digit tip regeneration in various mammalian species, including mice (Muneoka et al., 2008), rats (Said et al., 2004), monkeys (Singer et al., 1987) and humans (Illingworth, 1974) have been described in previous studies. The mouse digit has become a useful model to study mammalian regeneration because of a number of factors, including the description of strain-specific variation in response (Chadwick et al., 2007) and the identification of a regeneration defective mutant line (Han et al., 2003). In addition, failed regenerative responses resulting from proximal digit amputation have been characterized in a number of recent studies (Agrawal et al., 2009; Gourevitch et al., 2009; Wang et al., 2010), and the first stimulation of an induced regenerative response from a non-regenerating amputation injury has recently been demonstrated (Yu et al., 2010). In the current study we provide a detailed

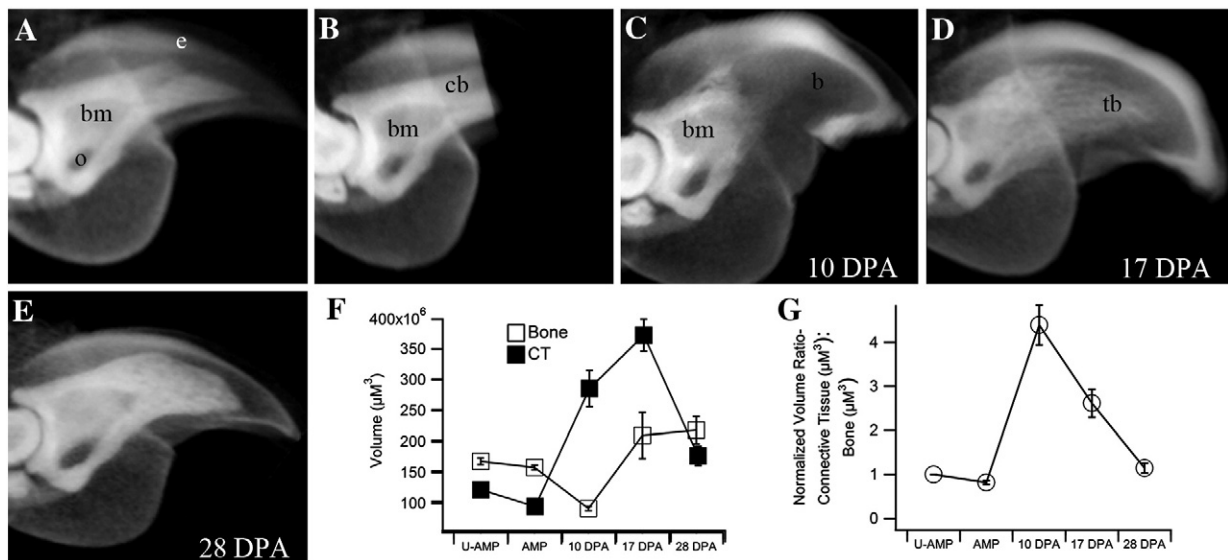


**Fig. 4.** Volumetric micro-CT analysis of regeneration. Digits treated with a soft-tissue contrast agent made the epidermis radio-opaque and enabled analyses of soft tissue versus bone volume during regeneration. (A) The intact digit tip shows the bone marrow cavity (bm), os hole (o) and epidermis (e). (B) Immediately after amputation the digit stump contains cortical bone (cb) distal to the bone marrow cavity. (C) At 10 DPA the distal cortical bone has eroded and the bone marrow cavity is contiguous with the distal digit blastema (b). (D) At 17 DPA the regenerated trabecular bone (tb) appears as a loose network of bony tissue with a non-uniform density. (E) At 28 DPA the regenerated bone density is enhanced. The general structure of the regenerate is similar but not identical to the original (compare A and E). (F) A plot of bone (open squares) versus soft tissue (ct, solid squares) volume shows a sharp increase in the soft tissue and a decrease in bone associated with digit blastema formation. The final volume of both soft tissue and bone is significantly higher in the 28 DPA regenerate as compared to the original digit tip. (G) Normalizing the ratio of soft tissue to bone volume during the regeneration process shows a spike associated with digit blastema formation and an eventual return to normal levels.

characterization of endogenous digit tip regeneration in adult outbred mice, and our findings confirm and extend previous observations.

#### *Wound healing*

The regeneration of various vertebrate limb structures can be described in terms of distinct stages beginning with an initial wound healing period that is followed by the formation of a blastema, and concluding with the re-differentiation of structural tissues (Gardiner et al., 2002; Muneoka et al., 2008). The regeneration of the neonatal digit tip has been well characterized (Han et al., 2008; Yu et al., 2010) and shares general characteristics with the adult regenerative response (Neufeld and Zhao, 1995). One distinction between neonatal and adult digit tip regeneration is the amount of time required to complete the regeneration response and, as well, the length of time spent in the various regeneration stages. The wound healing stage in adult regeneration is prolonged and characterized by a slow but highly variable time to complete wound closure. There are a number of events associated with the wound healing phase of adult regeneration that are noteworthy and linked to the variability in the timing of blastema formation. First, the epidermis does not close across the amputated bone surface even if the amputation is made at a very distal level where the amputation surface area is small. Instead, the wound epidermis seals the injury site by attaching to the lateral rim of the amputated bone. The bone stump does not appear to be a physical barrier to wound closure because the dorsal epidermis associated with the nail extends distal to the amputation plane and folds back proximally to remain in contact with the lateral bone surface. The inability of injured epidermis to migrate across the amputated bone surface is novel and identifies a unique characteristic of the amputation wound that distinguishes it from more traditional mammalian skin wounds.

A second remarkable aspect of the wound healing stage is that there is extensive degradation of the stump bone. Bone degradation following digit tip amputation has been previously noted in both adult and neonatal regeneration (Han et al., 2008; Revardel and Chebouki, 1986). The erosion of bone appears to be largely localized to the distal stump and, because of the inability of the epidermis to close over the bone stump, wound closure is delayed until the bone erosion response is completed. Thus, by the time wound closure is completed, roughly 50% of the terminal phalangeal bone volume is lost, and the regeneration blastema forms from a level that is more proximal to the original amputation plane. Histological evidence indicates that the bone degradation response is associated with an enhanced level of osteoclasts that is triggered by the amputation injury and associated with the stump bone. Enhanced osteoclast activity is noted in association with new bone formation during bone fracture repair (Gerstenfeld et al., 2003; Schell et al., 2006; Schindeler et al., 2008) however; in this case bone erosion and osteogenesis are occurring concurrently whereas in digit regeneration the degradation and osteogenic responses are temporally delineated and non-overlapping.

#### *Blastema formation*

The formation of the digit blastema during adult regeneration occurs rapidly once the bone degradation response is completed and the wound epidermis closes. Analyzing blastema stages using traditional histology and microCT provides clear evidence that digit blastema formation is associated with the bone degradation response, with the proximal blastema forming in the region of the eroded stump bone. In amphibian blastema formation, proteolytic digestion of stump tissues is associated with the release of cells that enter the blastema (Kato et al., 2003; Miyazaki et al. 1996; Vinarsky et al., 2005; Yang and Bryant, 1994; Yang et al., 1999). Similarly, the extensive amount of bone erosion associated with adult digit tip regeneration

provides a mechanism that exposes the bone marrow to the injury site allowing for the involvement of bone marrow derived stem and/or bone progenitor cells in blastema formation.

Classic studies of the regenerating salamander limb show that, by comparison to mature tissue, the blastema is largely devoid of blood vessels (Mescher and Cox, 1988; Munaim and Mescher, 1986). Ink injection and resin casts studies in rats and mice suggest that digit tip regeneration is similarly associated with a reduced level of vasculogenesis (Said et al., 2004). Our finding that the majority of CD31<sup>+</sup> cells in the digit blastema are single cells, and that their frequency is significantly reduced by comparison to mature non-regenerating tissues is consistent with the conclusion that the digit blastema is characterized by reduced vascularity. We also find that the majority of endothelial cells in both non-regenerating and regenerating digit tissue co-express SCA-1, a putative endothelial progenitor cell marker (Orimo et al., 2005). Interestingly, the majority of SCA-1 expressing cells in the mature and regenerating digit are associated with the endothelial lineage suggesting that the role SCA-1<sup>+</sup> cells play in digit tip regeneration is linked to the vascular response. This conclusion is consistent with the results of studies on the wound healing response following digit amputation at a proximal level (non-regenerating) showing both enhanced vascularization (Said et al., 2004) and a prevalence of SCA-1<sup>+</sup> cells (Agrawal et al., 2009).

#### *Redifferentiation*

In adult and juvenile rodents, the regenerative response results in near perfect restoration of digit morphology (Borgens, 1982; Revardel and Chebouki, 1986; Neufeld and Zhao, 1995). Unlike most regenerating model systems, the mouse neonatal digit tip does not undergo redifferentiation by following a process of redevelopment, but instead regenerates bone by direct intramembranous ossification (Han et al., 2008), and we confirm here that the adult digit follows a similar mode of ossification. The ossification response results in the regeneration of a trabecular bone framework that increases in bone density with time, and establishes a smooth interface with the stump cortical bone. Our histological measurements indicate that the P3 bone returns to its original length, however the regenerated bone volume is significantly larger than unamputated controls. Defects in the precision of the regeneration response has also been observed in neonatal regenerates and this, along with an ossification profile that deviates from digit development (Han et al., 2008), provides evidence that digit tip regeneration represents an example of an evolved regenerative response (Muneoka et al., 2008; Yu et al., 2010).

#### *Re-amputation and evolved regeneration*

The wound healing phase of the digit tip regeneration response is highly dynamic and involves the erosion of distal bone followed by epidermal closure at a more proximal level. This injury induced re-amputation response is novel and suggestive of an evolved injury response that is linked to mechanisms controlling the regenerative response. This re-amputation response is not an autotomy response in which a body part is self-amputated to avoid predation, but there are some similarities. The best characterized autotomy response involves the spontaneous level-specific self-amputation of the tail in lizards that is followed by a regenerative response that replaces the original tail with an imperfect replica (Clause and Capaldi, 2006; Bellairs and Bryant, 1985). In lizard tail autotomy there are two independent aspects for the evolution of the response. The first is the obvious predator/prey survival factor associated with the self-amputation response itself, and the second involves the pre-determined amputation levels that facilitate the regenerative response (Bellairs and Bryant, 1985). These two events are not necessarily linked since autotomy of tails to escape predation without an ensuing regenerative response has been described (Schargal et al., 1999). The response of



the digit tip is not a spontaneous self-amputation, however it is a novel injury induced self-amputation that leads to blastema formation and a regenerative response. Since there is mounting evidence that regenerative responses have evolved independently in distinct phylogenetic groups (Muneoka et al., 2008; Bely and Sikes, 2010; Garza-Garcia et al., 2010), we propose that the re-amputation response following injury to the distal digit tip evolved as a necessary modification of the wound healing response to ensure a successful regenerative response.

We propose that survival following traumatic injury such as amputation represents a selective pressure that can drive the evolution of wound healing mechanisms toward the acquisition of a regenerative response. The diversity of digit structures among tetrapod vertebrates lends support to the notion that digits play a key role in limb function, and that the ability to regenerate terminal structures of digits is critical for survival. We are intrigued by the observation that digit tip regeneration appears to involve an interaction between cells of the connective tissue surrounding the terminal phalanx and cells derived from the bone marrow (see also Han et al., 2008). If this interaction is required for a regenerative response, then the degradation of bone represents a target for positive selection since it provides a way for marrow-derived cells to enter the wound and participate in blastema formation. These observations suggest that the extreme distal amputation wound is not regeneration competent, whereas a more proximal amputation injury involving the bone marrow cavity is, thus a self-inflicted re-amputation response evolved as a necessary pre-condition for mounting a regeneration response. Consistent with conclusions derived from regeneration studies on invertebrates and amphibians (Bely and Sikes, 2010; Garza-Garcia et al., 2010), our studies on mammalian digit regeneration provide evidence that mechanisms driving a regenerative response is under positive selective pressures.

In order to effect successful regeneration, we predict that the injury wound must fulfill four specific criteria. The first is that the wound itself must be permissive for a regenerative response. The wound epidermis is generally recognized as creating an environment at the amputation wound that is critical for a regenerative response (Bryant et al., 2002; Han et al., 2005), and the formation of a wound epidermis across the amputation injury is an essential first step. During digit tip regeneration, the inability of the epidermis to close across the amputated distal bone delays the regenerative response until osteoclast driven bone erosion is completed and wound closure creates a regeneration-permissive wound environment. Second, the regenerating wound must contain cells that have the potential to participate in re-building the structural components of the regenerate, and in the case of digit tip regeneration, multipotent stem cells present in the bone marrow are likely candidates to serve this function (Wu et al., 2007). Third, the coordination of pattern during the regeneration process plays an important role in dictating the morphology of the regenerate, thus the involvement of cells that possess positional information is a key component in any regenerative response. Studies in salamanders and humans provide evidence that connective tissue fibroblasts maintain positional memory (Chang, 2009; Bryant et al., 1987) and, in salamanders, these cells are intricately involved in both contribution and pattern formation during limb regeneration (Gardiner et al., 2002). During digit tip regeneration the connective tissue cells that surround the P3 element represent a potential source for cells critical for patterning the regenerative response. Fourth, a functional interface between the mature tissues of the stump and the newly forming tissues of the regenerate must be restored. In digit tip regeneration, we propose the erosion of bony tissue during wound healing serves an additional role in preparing the stump tissue for establishing such a functional interface. It seems equally likely that the erosion of stump tissues during amphibian limb regeneration functions both in releasing cells to the

regeneration response and as well in preparing the stump/regenerate interface.

## Acknowledgments

We thank members of the Muneoka lab for discussions. We thank Albert McManus and Jon Mogford for critical input. We are grateful to Luis Marrero for training in immunohistochemistry. Research funded by grants R01HD043277 from the NIH, W911NF-06-1-0161 from DARPA and the John L. and Mary Wright Ebaugh Endowment Fund at Tulane University.

## References

- Agrawal, V., Johnson, S.A., Reing, J., Zhang, L., Tottey, S., Wang, G., Hirschi, K.K., Brauhut, Gudas, L.J., Badyrak, S.F., 2009. Epimorphic regeneration approach to tissue replacement in adult mammals. *PNAS* 107, 3351–3355.
- Bellairs, A.D.A., Bryant, S.V., 1985. Autotomy and Regeneration in Reptiles. In: Gans, C., Billett, F. (Eds.), *Biology of the Reptilia*. John Wiley and Sons, Inc, p. 15B.
- Bely, A.E., Sikes, J.M., 2010. Latent regeneration abilities persist following recent evolutionary loss in asexual annelids. *PNAS* 107, 1464–1469.
- Bolon, B., Morony, S., Cheng, Y., Hu, Y.L., Feige, U., 2004. Osteoclast numbers in Lewis rats with adjuvant-induced arthritis: identification of preferred sites and parameters for rapid quantitative analysis. *Vet. Pathol.* 41, 30–36.
- Borgens, R.B., 1982. Mice regrow the tips of their foretoes. *Science* 217, 747–750.
- Bryant, S.V., Endo, T., Gardiner, D.M., 2002. Vertebrate limb regeneration and the origin of limb stem cells. *Int. J. Dev. Biol.* 46, 887–896.
- Bryant, S.V., Gardiner, D.M., Muneoka, K., 1987. Limb development and regeneration. *Am. Zool.* 27, 675–696.
- Chadwick, R.B., Bu, L., Yu, H., Hu, Y., Wergedal, J.E., Mohan, S., Baylink, D.J., 2007. Digit tip regrowth and differential gene expression in MRL/MpJ, DBA/2, and C57BL/6 mice. *Wound Repair Regen.* 15, 275–284.
- Chang, H.Y., 2009. Anatomic demarcation of cells: genes to patterns. *Science* 326, 1206–1207.
- Clause, A.R., Capaldi, E.A., 2006. Caudal autotomy and regeneration in lizards. *J. Exp. Zool. Comp. Biol.* 305, 965–973.
- Garza-Garcia, A.A., Driscoll, P.C., Brookes, J.P., 2010. Evidence for the local evolution of mechanisms underlying limb regeneration in salamanders. *Integr. Comp. Biol.* 1–8 doi: 10.1093/icb/icq022. Advance Access published April 21, 2010.
- Gardiner, D.M., Endo, T., Bryant, S.V., 2002. The molecular basis of amphibian limb regeneration: integrating the old with the new. *Semin. Cell Dev. Biol.* 13, 345–352.
- Gerstenfeld, L.C., Cullinane, D.M., Barnes, G.L., Graves, D.T., Einhorn, T.A., 2003. Fracture healing as a post-natal developmental process: molecular, spatial, and temporal aspects of its regulation. *J. Cell. Biochem.* 88, 873–884.
- Gourevitch, D.L., Clark, L., Bedelbaeva, K., Leferovich, J., Heber-Katz, E., 2009. Dynamic changes after murine digit amputation: the MRL mouse digit shows waves of tissue remodeling, growth, and apoptosis. *Wound Repair Regen.* 17, 447–455.
- Han, M., Yang, X., Farrington, J.E., Muneoka, K., 2003. Digit regeneration is regulated by *Mx1* and *BMP4* in fetal mice. *Development* 130, 5123–5132.
- Han, M., Yang, X., Lee, J., Allan, C.H., Muneoka, K., 2008. Development and regeneration of the neonatal digit tip in mice. *Dev. Biol.* 315, 125–135.
- Han, M., Yang, X., Taylor, G., Burdsal, C.A., Anderson, R.A., Muneoka, K., 2005. Limb regeneration in higher vertebrates: developing a roadmap. *Anat. Rec. B New Anat.* 287, 14–24.
- Holmes, C., Stanford, W.L., 2007. Concise review: stem cell antigen-1: expression, function, and enigma. *Stem Cells* 25, 1339–1347.
- Illingworth, C.M., 1974. Trapped fingers and amputated finger tips in children. *J. Pediatr. Surg.* 9, 853–858.
- Kalluri, R., Zeisberg, M., 2006. Fibroblasts in cancer. *Nat. Rev. Cancer* 6, 392–401.
- Kato, T., Miyazaki, K., Shimizu-Nishikawa, K., Koshida, K., Obara, M., Mishima, H.K., Yoshizato, K., 2003. Unique expression patterns of matrix metalloproteinases in regenerating newt limbs. *Dev. Dyn.* 226, 366–376.
- Mescher, A.L., Cox, C.A., 1988. Hyaluronate accumulation and nerve-dependent growth during regeneration of larval *Ambystoma* limbs. *Differentiation* 38, 161–168.
- Metscher, B.D., 2009. MicroCT for developmental biology: a versatile tool for high-contrast 3D imaging at histological resolutions. *Dev. Dyn.* 238, 632–640.
- Miyazaki, K., Uchiyama, K., Imokawa, Y., Yoshizato, K., 1996. Cloning and characterization of cDNAs for matrix metalloproteinases of regenerating newt limbs. *Proc. Natl. Acad. Sci. USA* 93, 6819–6824.
- Muller, T.L., Ngo-Muller, V., Reginelli, A., Taylor, G., Anderson, R., Muneoka, K., 1999. Regeneration in higher vertebrates: limb buds and digit tips. *Semin. Cell Dev. Biol.* 10, 405–413.
- Munaim, S.I., Mescher, A.L., 1986. Transferrin and the trophic effect of neural tissue on amphibian limb regeneration blastemas. *Dev. Biol.* 116, 138–142.
- Muneoka, K., Allan, C.H., Yang, X., Lee, J., Han, M., 2008. Mammalian regeneration and regenerative medicine. *Birth Defects Res. C Embryo Today* 84, 265–280.
- Neufeld, D.A., Zhao, W., 1995. Bone regrowth after digit tip amputation in mice is equivalent in adults and neonates. *Wound Repair Regen.* 3, 461–466.
- Newman, P.J., Berndt, M.C., Gorski, J., White II, G.C., Lyman, S., Paddock, C., Muller, W.A., 1990. PECAM-1 (CD31) cloning and relation to adhesion molecules of the immunoglobulin gene superfamily. *Science* 247, 1219–1222.

- Orimo, A., Gupta, P.B., Sgroi, D.C., Arenzana-Seisdedos, F., Delaunay, T., Naeem, R., Carey, V.J., Richardson, A.L., Weinberg, R.A., 2005. Stromal fibroblasts present in invasive human breast carcinomas promote tumor growth and angiogenesis through elevated SDF-1/CXCL12 secretion. *Cell* 121, 335–348.
- Reginelli, A.D., Wang, Y.Q., Sassoon, D., Muneoka, K., 1995. Digit tip regeneration correlates with regions of *Msx1* (*Hox 7*) expression in fetal and newborn mice. *Development* 121, 1065–1076.
- Revardel, J.L., Chebouki, F., 1986. Etude de la reponse à l'amputation des phalanges chez la souris: rôle morphogénétique des épithéliums, stimulation de la chondrogenèse. *Can. J. Zool.* 65, 3166–3176.
- Said, S., Parke, W., Neufeld, D.A., 2004. Vascular supplies differ in regenerating and nonregenerating amputated rodent digits. *Anat. Rec. A Discov. Mol. Cell. Evol. Biol.* 278, 443–449.
- Schargal, E., Rath-Wolfson, L., Kronfeld, N., Dayan, T., 1999. Ecological and histological aspects of tail loss in spiny mice with a review of its occurrence in rodents. *J. Zool. Lond.* 249, 187–193.
- Schell, H., Lienau, J., Epari, D.R., Seebeck, P., Exner, C., Muchow, S., Bragulla, H., Haas, N.P., Duda, G.N., 2006. Osteoclastic activity begins early and increases over the course of bone healing. *Bone* 38, 547–554.
- Schindeler, A., McDonald, M.M., Bokko, P., Little, D.G., 2008. Bone remodeling during fracture repair: the cellular picture. *Semin. Cell Dev. Biol.* 19, 459–466.
- Singer, M., Weckesser, E.C., Géraudie, J., Maier, C.E., Singer, J., 1987. Open finger tip healing and replacement after distal amputation in rhesus monkey with comparison to limb regeneration in lower vertebrates. *Anat. Embryol. Berl.* 177, 29–36.
- Vaananen, H.K., Zhao, H., Mulari, M., Halleen, J.M., 2000. The cell biology of osteoclast function. *J. Cell Sci.* 113 (Pt 3), 377–381.
- Vinarsky, V., Atkinson, D.L., Stevenson, T.J., Keating, M.T., Odelberg, S.J., 2005. Normal newt limb regeneration requires matrix metalloproteinase function. *Dev. Biol.* 279, 86–98.
- Wang, G., Badylak, S.F., Heber-Katz, E., Braunhut, S.J., Gudas, L.J., 2010. The effects of DNA methyltransferase inhibitors and histone deacetylase inhibitors on digit regeneration in mice. *Regen. Med.* 5, 201–220.
- Woodfin, A., Voisin, M.B., Nourshargh, S., 2007. PECAM-1: a multi-functional molecule in inflammation and vascular biology. *Arterioscler. Thromb. Vasc. Biol.* 27, 2514–2523.
- Wu, Y., Wang, J., Scott, P.G., Tredget, E.E., 2007. Bone marrow-derived stem cells in wound healing: a review. *Wound Repair Regen.* 15 (Suppl 1), S18–S26.
- Yang, E.V., Gardiner, D.M., Carlson, M.R.J., Nugas, C.A., Bryant, S.V., 1999. Expression of *Mmp-9* and related matrix metalloproteinase genes during axolotl limb regeneration. *Dev. Dyn.* 216, 2–9.
- Yang, E.V., Bryant, S.V., 1994. Developmental regulation of a matrix metalloproteinase during regeneration of axolotl appendages. *Dev. Biol.* 166, 696–703.
- Yu, L., Han, M., Yan, M., Lee, E.C., Lee, J., Muneoka, K., 2010. BMP signaling induces digit regeneration in neonatal mice. *Development* 137, 551–559.